One-step synthesis of gold nanoflowers of tunable size and absorption wavelength in the red & deep red range for SERS spectroscopy

Mathias Pacaud, Katel Hervé-Aubert, Martin Soucé, Alaa Abdelrahman Makki, Franck Bonnier, Amir Fahmi, Alexey Feofanov, Igor Chourpa

One-step synthesis of gold nanoflowers of tunable size and absorption wavelength in the red & deep red range for SERS spectroscopy

Mathias Pacaud,[a,b] Katel Hervé-Aubert,[a] Martin Soucé,[a] Alaa Abdelrahman Makki,[a] Franck Bonnier,[a] Amir Fahmi,[b] Alexey Feofanov [c,d] and Igor Chourpa*[a]

[a] EA6295 Nanomédicaments et Nanosondes, Université de Tours, Tours, France.

[b] Faculty Technology&Bionics, Rhein-Waal University of Applied Sciences, Kleve, Germany.

[c] Shemyakin and Ovchinnikov Institute of Bioorganic Chemistry, Russian Academy of Sciences, Moscow, Russia.

[d] Biological Faculty, Lomonosov Moscow State University, Moscow, Russia.

Supporting information for this article is given via a link at the end of the document.

*Corresponding Author at: UFR de Pharmacie, 31 Avenue Monge, F-37200, France.

E-mail address: Igor.chourpa@univ-tours.fr.

Keywords: gold nanoflower AuNF, surface plasmon resonance (LSPR) band, surface-enhanced Raman scattering (SERS) spectroscopy

Abstract:

We describe a novel protocol for a one-step, seed-less, organic solvent- and surfactant-free synthesis of optically dense aqueous colloids of gold nanoflowers (AuNF), with tunable absorption wavelength between 620 and 800 nm. We demonstrate that simple variation of the ratio of two reagents allows the plasmonic band position to be tuned to any desired wavelength ±5 nm, namely to those of the laser sources commonly used for SERS spectroscopy. The AuNF size distribution was sufficiently narrow, comparable to that known with seed-mediated synthesis. The AuNFs have been validated as efficient aggregation-free substrates for surface-enhanced Raman scattering (SERS) spectroscopy using two common fluorescent dyes, Nile Blue and Crystal Violet, both thiol-free. Their fluorescence was quenched and SERS signal intensity was a linear function of the dye concentration, from nanomolar to micromolar range. Easy to prepare and to use, these AuNFs appear as a particularly user-friendly and efficient way to obtain plasmonic substrate for SERS in the red and deep red spectral range.

1. Introduction

Gold nanoflowers (AuNF) have emerged during the past decade as novel plasmonic nanosystems absorbing light in the red - deep red range (600-900 nm, a part of the "tissue optical window" between 600 and 1200 nm) [1-3]. The AuNF are interesting for many applications [4, 5], in particular as agents for photoinduced heating and substrates for surface-enhanced Raman scattering (SERS) spectroscopy [6]. Due to its high sensitivity, molecular specificity and selectivity, SERS spectroscopy is a rapidly developing analytical and bio-analytical technique. SERS excitation in the 630-850 nm region is favourable for bio-analytical SERS applications, because this wavelength range allows a compromise between minimal light interaction with biological tissues [1, 2] and the good performance of laser sources and CCD detectors [3].

The SERS effect is observed for organic molecules situated in the vicinity of a nanostructured surface of a noble metal, often in the form of nanoparticles (NP), which displays collective oscillations of surface electrons called plasmons [6]. The SERS effect implies that the excitation wavelength coincides with the localized surface plasmon resonance (LSPR) band of the noble metal NP. Since isotropic smooth AuNP have their LSPR band around 530 nm, their use for SERS with higher wavelength excitation sources is possible only in the case of NP aggregation. For aggregation-free LSPR absorption in the red-deep red range, anisotropic gold nanosystems like nanorods (AuNR), nanostars (AuNS) and nanoflowers (AuNF) are being developed [4, 5, 7-13]. It has to be noted that the morphology of some short-tipped AuNS is very similar to that of AuNF. Unfortunately, AuNR and some long-spiked AuNS may have an intrinsical biotoxicity [7], due to their morphology [8] and/or due to the presence of surfactants like cetrimonium bromide (CTAB) employed in their formulation. Indeed, surfactant-free AuNS synthesized by Yuan et al. [9] had reduced toxicity and permitted an easy surface functionalization. Thus, surfactant-free synthesis of AuNF has to be preferred for applications like biosensing.

Although a certain number of protocols of generating AuNF and AuNS has been reported by various research groups [4, 9-13] they typically involve at least two synthesis steps, corresponding to a nucleation-growth mechanism [14, 15]. The first step consists in introducing some seeds (silver [12], gold [9] or magnetic NPs [10] of diameters ca. 5 nm), either synthesized independently or in situ. Nucleation of silver and gold seeds is usually reached with one of the stronger reducing agents such as $NaBH_4$ [4, 5]. The second synthesis step is intended to favour slow anisotropic growth of AuNF or AuNS around the seeds, using a mild reducing agent like ascorbic acid or hydroxylamine. Size, shape and surface properties are usually controlled by the amount and nature of reducing agents and their ratio to the Au precursor. Anisotropic Au nanosystems can be synthesized in the presence of organic solvents and/or of capping agents like silver or other metal ions, surfactant

molecules or polymers [4, 5]. The latter are intended to direct the anisotropic growth along specific crystallographic directions or to stabilize the surface. As a result, prior to use of those AuNF or AuNS for SERS, further post-synthesis steps are usually required, in order to remove the solvents, the excess of seeds and reagents [4, 5]. Only few seed-less [11] or surfactant-free [9, 12] approaches have been reported so far. For instance, He et al. [11] have proposed a one-pot seedless protocol for the synthesis of AuNS, using ascorbic acid in the presence of silver nitrate ($AgNO_3$). The group of Vo-Dinh have published a systematic study of well-controlled geometry and optical response of gold nanostars using silver seeds but without surfactant [12].

To the best of our knowledge, the protocols of AuNF synthesis without seeds nor surfactant are even less common. For instance, Jena and Raj [13] used 5-hydroxyindole-3-acetic acid to generate, at room temperature, flower-like gold nanoparticles of a large, ca. 150 nm size, surprisingly showing two absorption bands at 545 and 1250 nm. Thus, there is no 'gold standard method' and there is still a need of a more convenient, rapid and efficient protocol for seed-less and surfactant-free synthesis of AuNF of controlled size and tunable LSPR band position within the 600-800 nm range.
In response to this need, we propose here a novel one-step synthesis method based on a mild chemistry in aqueous medium at room temperature.

2. Materials and methods

2.1. Chemicals

Gold (III) chloride trihydrate ($AuHCl_4.3H_2O$) (≥ 99.9%), trisodium citrate dihydrate ($HOC(COONa)(CH_2COONa)_2 \cdot 2H_2O$) (≥ 99.0%), sodium hydroxide (NaOH) (≥ 97.0 %) and Crystal Violet were purchased from Sigma–Aldrich (Saint Quentin Fallavier, France). Hydroxylamine hydrochloride ($NH_2OH \cdot HCl$) (≥ 99.0%), and Polyvinylpyrrolidone (PVP, M_w 7,000 - 11,000) were purchased from VWR (Fontenay-sous-Bois, France) and BASF (Levallois-Perret, France), respectively. Nile blue A, pure certified, was purchased from Acros Organics, (New Jersey, USA). All the reagents were used without further purification. Ultrapure water (Milli-Q) was used for the preparation of all solutions.

2.2. AuNF synthesis

Gold nanoflowers synthesis was carried out as follows: to 20 mL of water under vigorous magnetic stirring, aqueous solutions of hydroxylamine (0.1 M, volumes 0.3, 0.4, 0.45, 0.54, 0.56 or

0.64 mL), trisodium citrate (0.1 M, 1.0 mL) and sodium hydroxide (0.01 M, volumes 1.0, 1.0, 0.9, 0.9, 0.8 or 0.8 mL) were added. Upon addition of a freshly prepared aqueous solution of $HAuCl_4$ (0.01 M; 1.0 mL), the initial colourless solution immediately turned dark blue. The resultant colloid was stirred for ca. 30 seconds and transferred to a hermetically closed tube protected from light with aluminium foil. The final solution was kept at 20 ± 1 °C. In some cases, 0.25 mL of PVP aqueous solution (final concentration 13.5 µM) were added for better stability of the colloids.

2.3. Instrumental

UV-visible absorption spectra were acquired using a Genesys 10S UV-vis spectrophotometer (Thermo Scientific, France).

IR spectra were acquired with a Frontier spectrometer (Perkin Elmer, France) equipped with a Quest multiple reflection diamond attenuated total reflectance (ATR) accessory (Specac, UK) using dried 2 µL drops of NF suspension and citrate solution.

TEM experiments were carried out on a transmission electron microscope JEOL JEM-1011 (JEOL Inc., Peabody, MA, USA) operating at an acceleration voltage of 100 kV. AuNF in aqueous suspension were deposited on carbon-coated Cu grids. Excess water was removed by filter paper. The obtained samples were left to dry under ambient air. Image J software was used to measure the size distribution of AuNF, and for each particle, two perpendicular dimensions were measured. For each batch, the weighted average size was determined as the center of mass of the corresponding size distribution, calculated according to the equation: $D = \frac{\sum D_i N_i}{\sum N_i}$ where D_i is AuNF dimension range (0-10 nm presented as 5 nm, 10-20 nm presented as 15 nm, … 140-150 nm presented as 145 nm), where N_i is the number of AuNF in the dimension range D_i.

The mean hydrodynamic diameter D_H values (z-average) were measured using dynamic light scattering (DLS, Malvern HPPS, Malvern Instruments, UK), at 25°C and with a He-Ne laser (4 mW, 633 nm, scatter angle 173°). Each measurement was done in triplicate.

The SERS spectra were recorded with a confocal Raman microspectrometer LabRam (Horiba SA, France) equipped with an EM CCD air-cooled detector, a 690 nm laser source (RO691-PLR45, Ondax Inc, Monrovia, CA, USA) providing 26.9 mW on the sample. The spectra were collected via a 10× objective focused on the top of the sample solution (200 µL) placed in a well of a P96 multiwell plate. The spectral data acquisition and treatment were done using a LabSpec software (Horiba SAS, Villeneuve d'Ascq, France).

3. Results and discussion

3.1. AuNF synthesis

Our protocol uses optimized quantities of well-known reagents that are typical for gold reduction (Scheme 1): hydroxylamine (NH_2OH, Solution 1) as a reductant, trisodium citrate ($Na_3Citrate$, Solution 2) as a stabiliser for particles, sodium hydroxide (NaOH, Solution 3) as a main pH regulator and tetrachloroauric(III) acid ($HAuCl_4$, Solution 4) as a gold precursor (see Materials and methods for more details). The reagent concentrations and volumes are easy to remember, as described below. First of all, aqueous solutions of all the reagents are prepared, at concentrations of 0.1 M for the Solutions 1 - 3 and 0.01 M for the Solution 4. The preparation is started by adding the Solutions 1 (0.3 - 0.65 mL), 2 (1 mL) and 3 (0.8 – 1 mL) to 20 mL of water under vigorous stirring at ambient temperature (21 ± 1 °C). The volumes of the Solutions 1 and 3 are varied in order to adjust the NH_2OH/NaOH molar ratio (hereafter called R) to the values of 0.3, 0.4, 0.5, 0.6, 0.7, 0.8. Then, 1 mL of the Solution 4 is injected into this mixture: the colourless solution immediately turns dark blue (Scheme 1A) and, after ca. 30 seconds, the stirring can be stopped. No washing steps are needed, the AuNF colloids are useable for SERS spectroscopy as is, and are chemically and physically stable for several days, till about a week for certain batches. Nevertheless, they have to be protected against light by aluminium foil and stored hermetically closed to minimize their oxidation.

In the context of the nucleation-growth mechanism described above, our rapid AuNF synthesis seems to correspond to almost instantaneous nucleation of seeds (Step 1 in Scheme 1B) followed by appearance of anisotropic structures (Step 2) and their fast growth to give nanoflowers (Step 3) with characteristic petal-like structures (Scheme 1 C). This rapid growth in presence of citrate and chloride anions adsorbed on the gold surface may be the reason of its anisotropic nature in the absence of silver ions and surfactants.

Variations in citrate or gold concentration around the optimum value (10:1 molar ratio) do not allow controlling the LSPR position. This behaviour is different from that described by Ji et al [16] who had shown that the $HAuCl_4/Na_3Ct$ ratio affected both the pH and the growth of isotropic gold nanocrystals at elevated temperatures. In our study, synthesis without any citrate leads to colloids of reddish colours, i.e. with the LSPR band below 600 nm. Therefore, the presence of citrate is mandatory for successful AuNF synthesis by our method.

3.2. AuNF characterisation

The ratio R is the most critical parameter that affects the LSPR band position. An increase in R from 0.3 to 0.8 leads to a red shift of the LSPR band from ca. 620 to ca. 800 nm (Fig. 1). Between 0.4 and 0.8, the LSPR shift is a nearly linear function of R (Fig. 1B) and it is possible to adjust the LSPR position to any of three wavelengths of the laser sources most widely used in bio-analytical spectroscopy: 633 nm (R=0.4), 690 nm (R=0.6) and 785 nm (R=0.8). The LSPR band position was reproducible with a ±5 nm variation. The maximum absorbance for these LSPR bands was between 1.4 and 1.7.

The pH plays a very important role in such a synthesis. During the reaction, it affects the reactivity of gold complexes [17] and therefore, the kinetics of nanocrystal nucleation and growth. The high pH conditions are known to be favourable for gold reduction. Prior to the addition of gold precursor, the pH of the solutions ranges from 11.5 to 10.6 as a function of R (0.3 to 0.8), as expected from the respective concentrations of $NH_2OH.HCl$ and NaOH.

After the AuNF synthesis, the final pH decreases for all the colloids, down to about 10.9 for R = 0.3 and to 6.7 for R = 0.8. This is in agreement with the fact that both auric acid dissociation and its reduction generate H^+ species [18]. Counting only dissociation of auric acid, pH should still remain well above 10, permitting a rapid onset of reaction. The H^+ ions liberated due to the redox reaction further lower pH, reaching almost neutral for conditions of high R. At all the pH values described above the citrate is in anionic form (trivalent or partially divalent) to be adsorbed on the gold surface, thus playing a role both in the AuNF growth and colloidal stability. The presence of citrates in the AuNF batches can be confirmed by the characteristic bands of citrates the IR spectra (Figure SI2).

According to transmission electron microscopy (TEM) data (Fig. 2), the red shift of the LSPR band corresponds to bigger AuNF with an increased size and/or number of the 'petals' giving them a flower-like morphology. Coupling of plasmons of neighbouring petals is supposed to favour formation of 'hot spots' where the SERS effect is particularly strong. As seen from the TEM images and the histograms in Fig. 2, the size distribution was narrower in the populations of smaller AuNFs. The centre of mass of the histograms corresponds to the size of 49, 56, 75 and 89 nm for the R values

of 0.3, 0.5, 0.6 and 0.8, respectively. The hydrodynamic diameter D_H (z-average data from DLS), which includes the hydration layers around AuNF, increases from ca. 84 nm to ca. 112 nm.

As noticed above, the colloids are stable for about a week. However, the AuNF batches of higher R (bigger size and lower pH) show more pronounced sedimentation with time and are more prone to aggregation with time.

It is possible to stabilize the colloids of AuNF for at least a month by post-synthesis addition of 13.5 µM of PVP. As shown in Fig S1 (SI), PVP reduces the absorbance at the long-wavelength side of the LSPR band, presumably due to re-dispersion of some aggregates. As expected, the effect of PVP on the LSPR band shape is more significant for the bigger AuNFs at nearly neutral pH (absorption maximum around 690 nm and above, Fig. SI 1A) while it has almost no effect for the colloids of smaller AuNF at higher pH (absorption maximum at 620-660 nm, Fig. SI 1B). While useful to store big AuNF colloids for an extended time, the post-synthesis addition of PVP was optional, taking into account the ease and rapidity of producing a fresh batch whenever needed.

3.3. Analytical validation of the AuNFs

For the SERS validation experiments with a 690 nm laser excitation, the most appropriate AuNFs have the LSPR band maximum at ca. 690 nm (R = 0.6, pH 7.2). For this validation, we intentionally selected chromophores void of thiol groups and therefore having much lower affinity to the gold surface than rhodamine [19] and thiolated dyes [20] often used in the literature.

The sample preparation for SERS on our AuNF is very convenient: a 10-fold dilution of the analyte solution in the AuNF colloid placed into a well of a 96-multiwell plate. In this manner, we successfully obtained SERS spectra of two blue dyes, Nile Blue and Crystal Violet (absorption maxima in water at 635 and 590 nm, respectively) (Fig. 3A).

It has to be underlined that added PVP did not give its own signal and did not change the SERS signal of the NB dye (Fig. 3B). This is true under both neutral and basic conditions. As expected the pH increase from neutral to basic conditions affects the relative intensity of SERS bands of NB and contributes to a decrease of the fluorescence background. The only effect noticeable with PVP was seen as a need of about 5-10 min delay after the NB incubation to observe an optimal SERS/fluorescence ratio. This time would correspond to the diffusion of the dye trough the polymeric layer prior to reach the gold surface.

This shows the interest of a substrate with a minimal presence of polymer or surfactant: (i) to reduce its effect on the adsorption and thus the detection of analytes [11] and (ii) to facilitate further post-functionalization with some molecules of interest.

On the AuNFs coated with PVP, the SERS intensity was a linear function of the NB dye concentration from nanomolar to micromolar range (Fig. 4A). Using a rapid SERS spectra acquisition (16x1 sec), we observed the detection limits situated in the nanomolar range (2.5 nM for NB – Fig.4B) while it was possible to go below using longer acquisition times. As shown in Fig.4B, the signal stays the same (the fingerprint bands are recognizable), just noise goes up on dilution.

4. Conclusions

In conclusion, the novel protocol we propose herein presents several significant advantages compared to those previously published for synthesis of AuNF: in addition to be facile and rapid (one-step, seed-less), it avoids the presence of organic solvents or surfactants and of other metals than gold. Moreover, our method permits to tune the size of AuNFs between 50 and 90 nm and the corresponding LSPR band position between 620 and 800 nm. The most critical parameter of the synthesis has been determined to be the hydroxylamine/NaOH molar ratio, which regulates both the reductant content and the pH. Obviously, for a good reproducibility of the data, the temperature has to be controlled, since it plays a role in the reaction kinetics. As noted above, AuNF were not formed without addition of citrate. Together with citrates, chloride ions binding to the surface may also be essential to the anisotropic structure of the surface. The surfactant-free colloids are stable in water for several days and addition of a low concentration of PVP improves their long-term stability without affecting their aggregation-free SERS activity for organic dyes with relatively low affinity for gold. We believe that such a user-friendly wet chemistry protocol for rapid synthesis of AuNF should have very promising perspectives for bio-analytical SERS spectroscopy as well as for other plasmonic methods in the red-deep red range.

Conflicts of interests disclosure

The author declares no conflict of interest.

Acknowledgements

The authors acknowledge funding from the following grants in the framework of the MINERVA project (ERA-NET RUS PLUS program): RFBR 16-54-76013 (Russia), 01DJ16019 (Germany) and MENESR N°321 (France). The authors are grateful to Dr. Stéphanie David for her help with

experimental design, to Julien Burlaud-Gaillard (the IBiSA Electron Microscopy Facility, University of Tours) for TEM images and to Hiba Chamekh for technical assistance.

References

[1] S.J. Norton, T. Vo-Dinh
Theoretical Models and Algorithms in Optical Diffusion Tomography
Biomedical Photonics Handbook, CRC Press LLC (2003) (ISBN 0-8493-1116-0, DOI: 10.1201/9780203008997).

[2] R. Weissleder
A clearer vision for *in vivo* imaging
Nature Biotechnol., 19 (**2001)**, pp. 316-317 (DOI: 10.1038/86684).

[3] A.Smith, M. C. Mancini, S. Nie
Bioimaging: second window for in vivo imaging
Nat Nanotechnol., 4 (2009), pp. 710-711 (DOI: 10.1038/nnano.2009.326).

[4] P.R. Sajanlal, T.S. Sreeprasad, A. K. Samal, T. Pradeep
Anisotropic nanomaterials: structure, growth, assembly, and functions
Nano Reviews 2 (**2011)**,Article 5883 (DOI: 10.3402/nano.v2i0.5883).

[5] X. Gong, Y. Bao, C. Qiu and C. Jiang
Individual nanostructured materials: fabrication and surface-enhanced Raman scattering
Chem. Commun., 48 (2012), pp. 7003-7018 (DOI: 10.1039/C2CC31603J).

[6] L.E. Jamieson, S.M. Asiala, K. Gracie, K. Faulds, D. Graham
Bioanalytical Measurements Enabled by Surface-Enhanced Raman Scattering (SERS) Probes
Annu Rev Anal Chem (Palo Alto Calif), 10, (2017), pp. 415-437 (DOI: 10.1146/annurev-anchem-071015-041557).

[7] I. Fratoddi, I. Venditti, C. Cametti, M.V. Russo
How toxic are gold nanoparticles? The state-of-the-art
Nano Res., 8 (2015), pp. 1771-1799 (DOI: 10.1007/s12274-014-0697-3).

[8] L. Rodriguez-Lorenzo, R.A. Alvarez-Puebla, F.J. Garcia de Abajo, L.M. Liz-Marzan
Surface Enhanced Raman Scattering Using Star-Shaped Gold Colloidal Nanoparticles
J. Phys. Chem. C, 114 (2010), pp. 7336-7340 (DOI: 10.1021/jp909253w).

[9] H. Yuan, C.G. Khoury, H. Hwang, C.M. Wilson, G.A. Grant, T. Vo-Dinh
Gold nanostars: surfactant-free synthesis, 3D modelling, and two-photon

photoluminescence imaging

Nanotechnology, 23 (2012), Article 075102 (DOI: 10.1088/0957-4484/23/7/075102).

[10] C. Li, T. Chen, I. Ocsoy, G. Zhu, E. Yasun, M. You, C.Wu, J. Zheng, E. Song, C.Z. Huang, W. Tan
Gold-Coated Fe_3O_4 Nanoroses with Five Unique Functions for Cancer Cell Targeting, Imaging and Therapy
Adv Funct Mater., 24 (2014)**,** pp. 1772-1780 (DOI: 10.1002/adfm.201301659).

[11] S. He, M.W.C. Kang, F.J. Khan, E.K.M. Tan, M.A. Reyes, J. C. Y. Kah
Optimizing gold nanostars as a colloid-based surface-enhanced Raman scattering (SERS) substrate
J. Opt., 17 (2015), Article 114013 (DOI: https://doi.org/10.1088/2040-8978/17/11/114013).

[12] A.S. De Silva Indrasekara, S.F. Johnson, R.A. Odion, T. Vo-Dinh
Manipulation of the Geometry and Modulation of the Optical Response of Surfactant-Free Gold Nanostars: A Systematic Bottom-Up Synthesis
ACS Omega., 3 (2018), pp. 2202-2210 (DOI: 10.1021/acsomega.7b01700).

[13] B. K. Jena, C. R. Raj
Seedless, Surfactantless Room Temperature Synthesis of Single Crystalline Fluorescent Gold Nanoflowers with Pronounced SERS and Electrocatalytic Activity
Chem. Mater., 20 (2008), pp. 3546-3548 (DOI: 10.1021/cm7019608).

[14] J. Turkevich, P.C. Stevenson, J. Hillier
A study of the nucleation and growth processes in the synthesis of colloidal gold
Discuss. Faraday Soc., 11 (1951), pp. 55-75 (DOI: 10.1039/DF9511100055).

[15] G. Frens
Controlled Nucleation for the Regulation of the Particle Size in Monodisperse Gold Suspensions
Nature Physical Science, 241, (1973), pp. 20-22 (DOI: 10.1038/physci241020a0).

[16] X. Ji, X. Song, J. Li, Y. Bai, W. Yang, X. Peng
Size Control of Gold Nanocrystals in Citrate Reduction: The Third Role of Citrate
J. Am. Chem. Soc., 129 (**2007)**, pp. 13939-13948 (DOI: 10.1021/ja074447k).

[17] D. V. Goia, E. Matijević
Tailoring the particle size of monodispersed colloidal gold
Colloids and Surfaces, A, 146 (1999), pp. 139-152 (DOI: 10.1016/S0927-7757(98)00790-0).

[18] V. Soni and R. N. Mehrotra
Kinetics and mechanism of oxidation of hydroxylamine by tetrachloroaurate(III) ion
Transition Metal Chemistry, 28 (2003), pp. 893–898 (DOI: 10.1023/A:1026330125535).

[19] A. Jaworska, T. Wojcik, K. Malek, U. Kwolek, M. Kepczynski, A.A. Ansary, S. Chlopicki, and M. Baranska
Rhodamine 6G conjugated to gold nanoparticles as labels for both SERS and fluorescence studies on live endothelial cells
Mikrochim. Acta, 182 (2015), pp. 119-127 (DOI: 10.1007/s00604-014-1307-5).

[20] M. Gühlke, Z. Heiner, J. Kneipp
Surface-Enhanced Raman and Surface-Enhanced Hyper-Raman Scattering of Thiol-Functionalized Carotene
J Phys Chem C Nanomater Interfaces, 120 (2016), pp. 20702-20709 (DOI: 10.1021/acs.jpcc.6b01895).

Figure Captions

Scheme 1: A. Schematic description of the AuNF synthesis in aqueous media and photograph of the final colloid (optical density between 1.4 and 1.7). B. Hypothetic mechanism of the synthesis including 3 steps: seed formation (Step 1), anisotropic structure initiation (Step 2) and growth to form AuNFs (Step 3). C. Schematic drawing of the petal-like morphology of an AuNF (left) compared to its TEM image (right).

Figure 1: (A) UV-vis spectra of AuNF synthesized using different R = NH_2OH/NaOH molar ratio. (B) The LSPR band position vs R.

Figure 2: Top: Selection of typical TEM images of AuNFs synthesized using R = 0.3, 0.5, 0.6 and 0.8. Bottom: size distribution histograms. The centre of mass of the respective histograms corresponds to the size of 49, 56, 75 and 89 nm.

Figure 3: A. Chemical structures of two dyes, Crystal Violet (CV) and Nile Blue (NB) and their SERS spectra obtained on AuNFs with R = 0.6. B. Comparison of the SERS spectra of NB on AuNFs in absence and in presence of PVP at basic and neutral aqueous solutions.

The dye concentration was 5 µM. Each spectrum is an average of 16 scans of 1 sec.

Figure 4: A. SERS intensity (area of Raman bands in the range between 250 and 1800 cm^{-1}) vs NB concentration, from 2.5 to 100 nM (from 2.5 to 20 nM in the inset). The data presented are averages of three independent measurements. B. Typical SERS spectra of NB at micromolar and nanomolar concentrations. The intensities are normalized and offset for easier comparison.

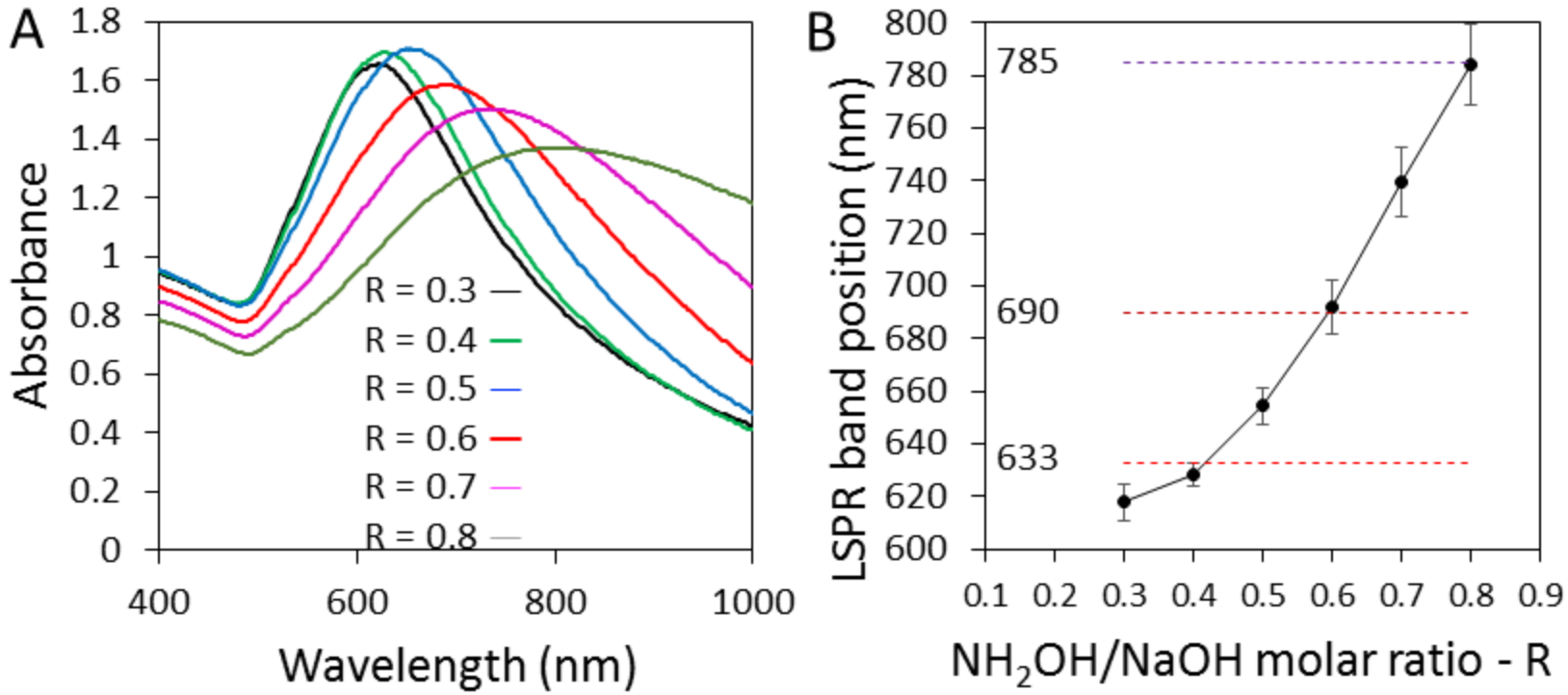
A
Absorbance
Wavelength (nm)
R = 0.3
R = 0.4
R = 0.5
R = 0.6
R = 0.7
R = 0.8
B
LSPR band position (nm)
785
690
633
NH2OH/NaOH molar ratio - R

Fig 1

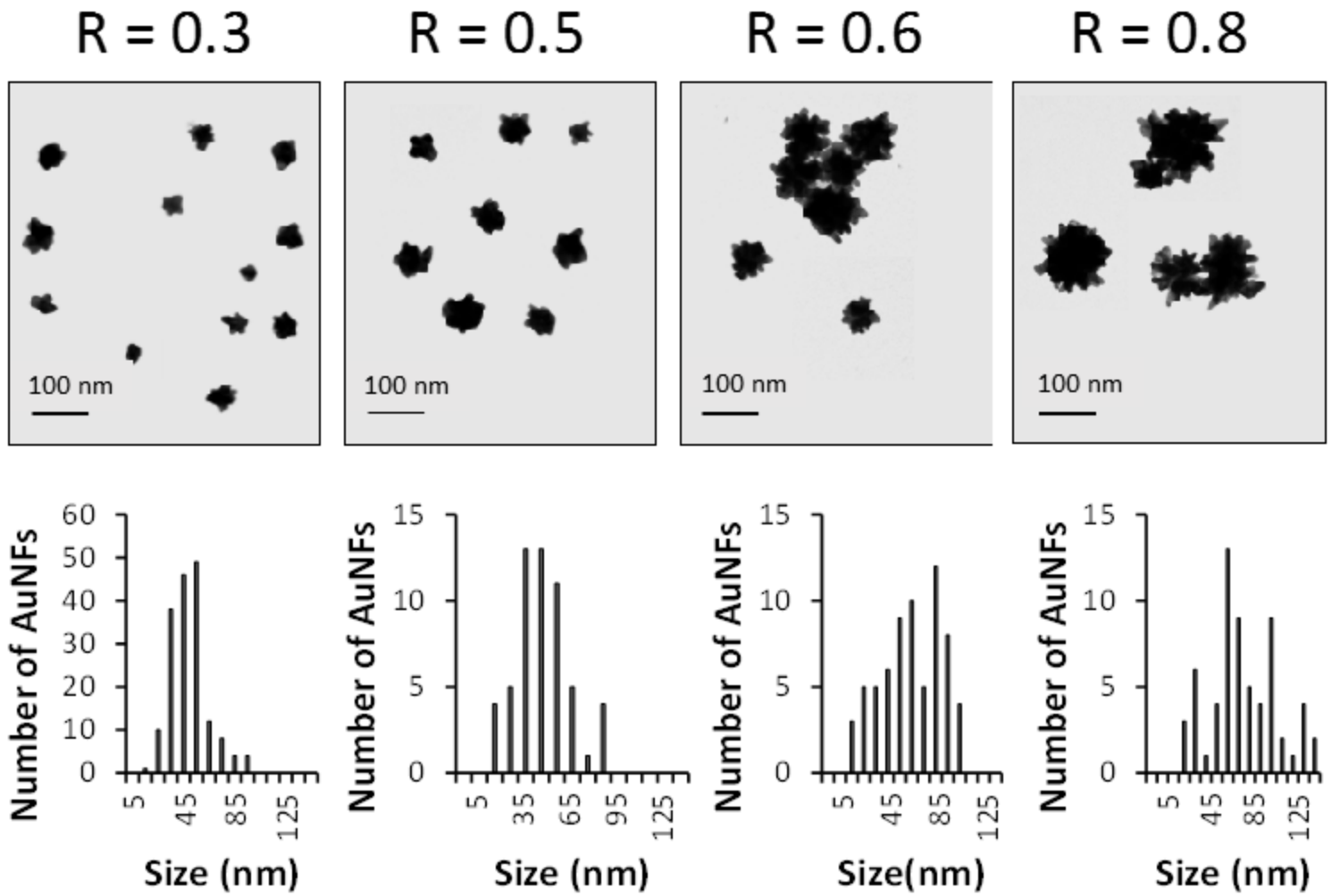
R = 0.3
R = 0.5
R = 0.6
R = 0.8
100 nm
100 nm
100 nm
100 nm
Number of AuNFs
Size (nm)
Number of AuNFs
Size (nm)
Number of AuNFs
Size(nm)
Number of AuNFs
Size (nm)

Fig 2

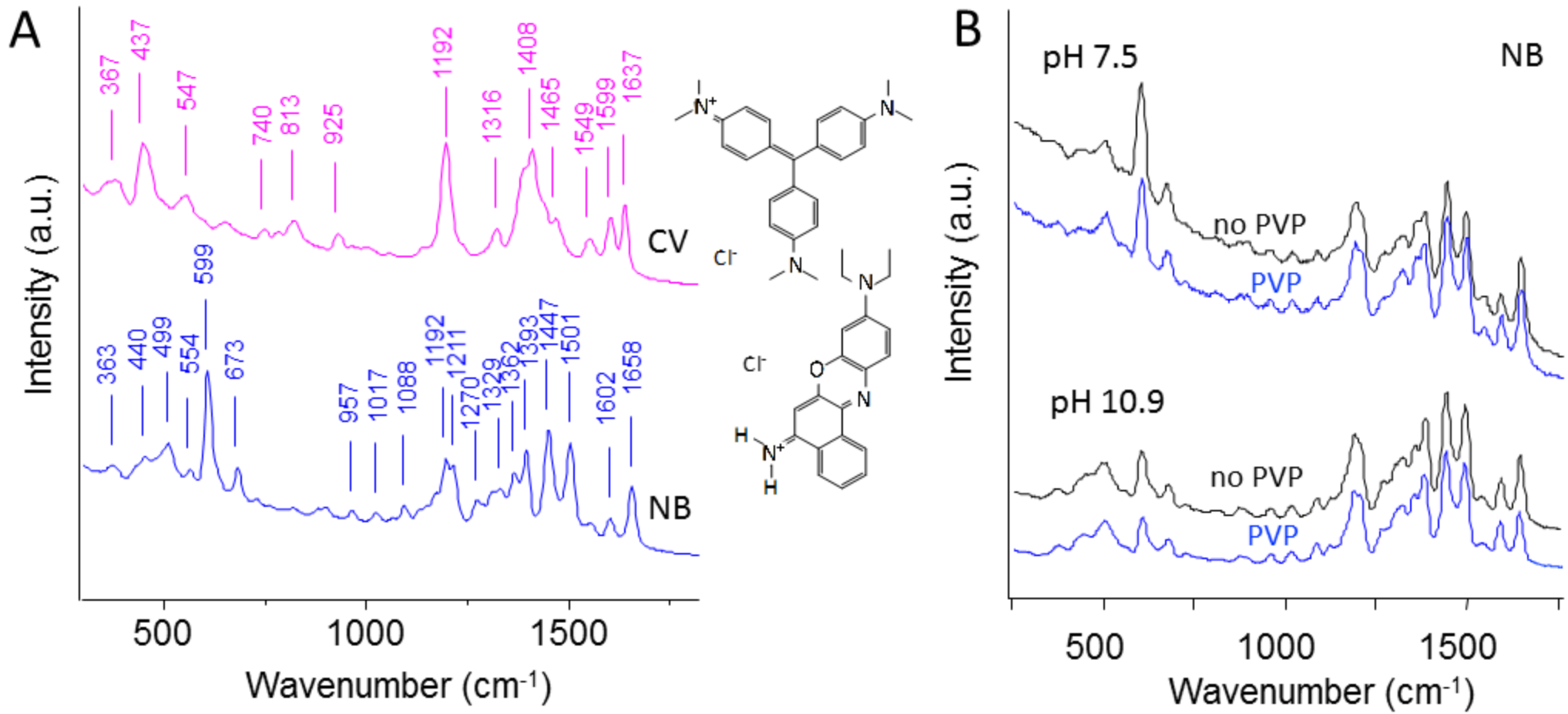
A
Intensity (a.u.)
367
437
547
740
813
925
1192
1316
1408
1465
1549
1599
1637
CV
599
363
440
499
554
673
957
1017
1088
1192
1211
1270
1329
1362
1393
1447
1501
1602
1658
NB
Cl-
Cl-
500
1000
1500
Wavenumber (cm-1)
B
pH 7.5
NB
no PVP
PVP
pH 10.9
no PVP
PVP
Intensity (a.u.)
500
1000
1500
Wavenumber (cm-1)

Fig 3

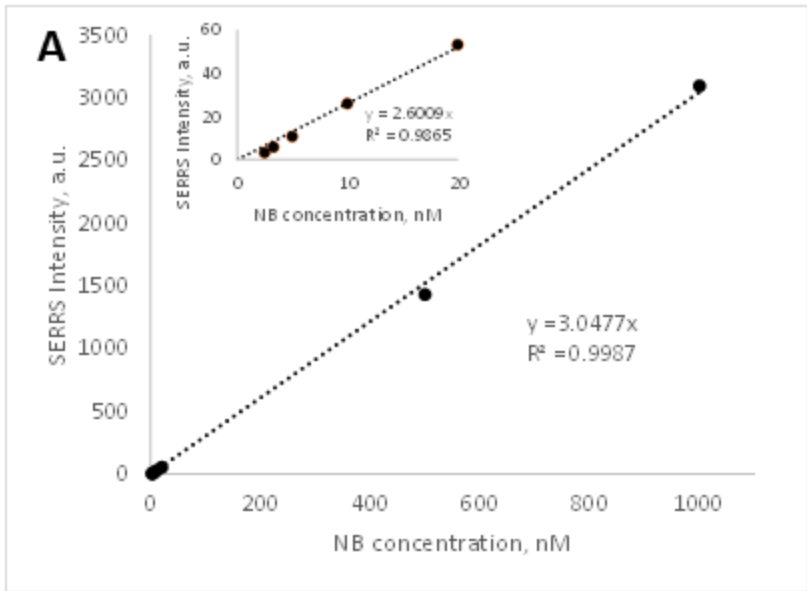
A
SERRS Intensity, a.u.
NB concentration, nM
y = 3.0477x
R² = 0.9987
y = 2.6009x
R² = 0.9865

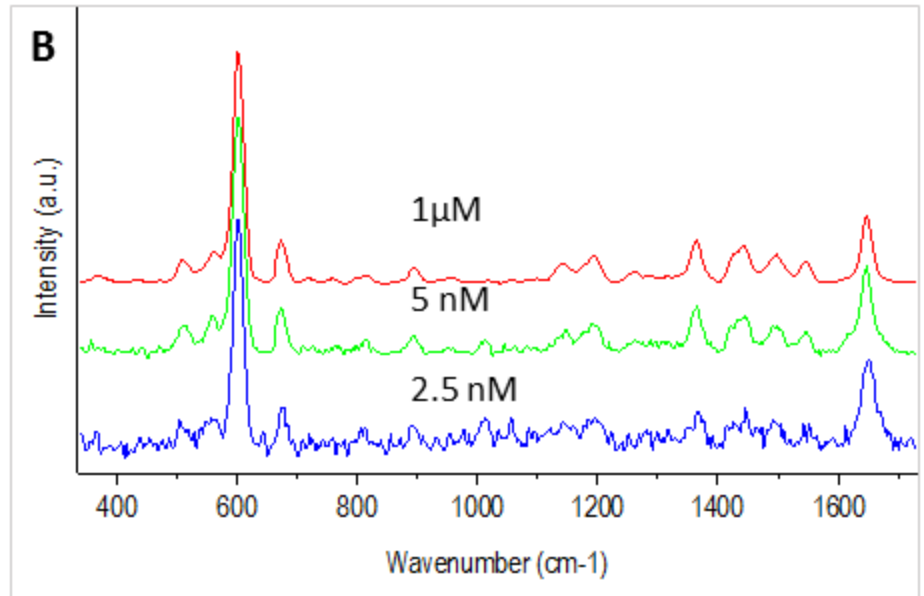
B
Intensity (a.u.)
1µM
5 nM
2.5 nM
Wavenumber (cm-1)

Fig 4

One step synthesis of AuNF for SERS in red-deep red range